

Technische Universität Dresden • Faculty of Mathematics

Diffusitivity of deformable cells

Master's thesis

to obtain the second degree

Master of Science
(M.Sc.)

written by

TIM VOGEL

(born on June 9, 2002 in FINSTERWALDE)

Day of submission: May 2, 2025

Supervised by Jun.-Prof. Dr. Markus Schmidtchen
(Institute of Scientific Computing)

Contents

1	Cell model	3
2	DF model dynamics	5
2.1	Area force	5
2.2	Edge force	7
2.3	Interior angle force	10
2.4	Overlap force	14
2.5	A simulation run	17
3	Sanity check	19

1 Cell model

The following two sections are a recap of the DF cell model and its dynamics that were introduced in my Bachelor's thesis [Vogel, 2023].

We are considering cells in the two dimensional space \mathbb{R}^2 . Here, cells are considered to be polygons.

Definition 1.1. Polygon

A polygon is a closed geometric figure in \mathbb{R}^2 , constructed by joining a finite number of straight line segments end to end. It can be described by a sequence of its vertices $(\vec{v}_1, \dots, \vec{v}_N)$. The following properties characterise a polygon:

1. A polygon is **simple** if no two line segments cross each other.
2. A polygon has a **positive orientation** if the vertices are ordered counter-clockwise.
3. A polygon has a **negative orientation** if the vertices are ordered clockwise.

Having established this definition, we are now ready to define our cell model.

Definition 1.2. Discrete form (DF)

A cell in its discrete form (DF) is given by an ordered sequence of its vertices $C = (\vec{v}_1, \dots, \vec{v}_N)$ if the resulting polygon when connecting every vertex with its neighbours and \vec{v}_1 with \vec{v}_N is simple and positively orientated. We set $\vec{v}_{N+1} = \vec{v}_1$ and $\vec{v}_0 = \vec{v}_N$ to enable periodic indexing, which simplifies the computation of the upcoming forces a lot.

In this thesis, DF cells may also be called discrete cells.

The next step is to describe the setup of a DF simulation.

Definition 1.3. DF simulation

A DF simulation considers $N_C \in \mathbb{N}$ cells. Each cell has the same amount of $N_V \in \mathbb{N}$ vertices. Thus, the notation of all cells and their vertices is given by

$$C^i = (\vec{v}_1^i, \dots, \vec{v}_{N_V}^i), \quad 1 \leq i \leq N_C.$$

The complete set of all cells is represented by

$$\vec{C} = (C^1, \dots, C^{N_C}),$$

which also contains all vertices from all cells.

The simulation's dynamics are defined on all cell vertices via the stochastic differential equation (SDE):

$$d\vec{v}_j^i(\vec{C}) = \mathbf{F}_j^i(\vec{C}) + \sqrt{2D}d\vec{B}^i, \quad 1 \leq i \leq N_C, \quad 1 \leq j \leq N_V.$$

where \mathbf{F}_j^i describes the total interaction force on vertex \vec{v}_j^i caused by the current cell system \vec{C} and $\sqrt{2D}d\vec{B}^i$ models the two dimensional standard Brownian motion of cell i with diffusion coefficient D . Note, that all vertices of cell i perform the same Brownian motion such that the whole cell i moves in the direction of \vec{B}^i .

The simulation domain is always a square around the origin that is defined by $L > 0$ via

$$\Omega_L = [-L, L]^2.$$

How the interaction force \mathbf{F} can be modelled will be shown the next chapter.

2 DF model dynamics

We characterise the interaction force \mathbf{F} as the sum of gradient flows of energies. A gradient flow describes how a system changes over time in a way that always reduces a given energy $E(\vec{C})$. To obtain the gradient flow of this energy on vertex \vec{v} , we must add the term $-\nabla_{\vec{v}}E(\vec{C})$ to \mathbf{F} . Since all our energy terms are positive, the lowest possible value is zero. So, the gradient flow moves the system step by step toward this minimum, always trying to decrease the energy until, ideally, it reaches zero. This is how we guide the motion of our cells: by letting them follow the gradient flow of each energy so that their shapes and vertex positions gradually adjust to reduce the total energy. In [Vogel, 2023], the area, edge, interior angle, and overlap energies were introduced. The first three energies are responsible for maintaining the shape of each cell. All of these three according forces act on each cell in a vacuum based only on its own current cell shape.

Interactions between different cells just arise from the overlap force, which acts to resolve overlaps and to prevent cell interpenetration. In the process of resolving overlaps, the shape of the cells will change. Once the overlap is resolved, the first three forces act to restore the cell's original shape.

The central question we aim to investigate in this thesis is how the deformability of individual cells influences the overall diffusivity of the cell system. But first, let us introduce each of the mentioned forces.

2.1 Area force

The area force is designed to maintain each cell's area close to a preferred target value. In order to compute a cell's area, which is the area of a positively orientated polygon, we can use the Shoelace formula.

Proposition 2.1. Shoelace formula for DF cells

Let $C = (\vec{v}_1, \dots, \vec{v}_N)$ be a DF cell with $\vec{v}_i = (v_i^1, v_i^2)^T$ for $i = 1, \dots, N$. We determine the area A_C of C by applying the Shoelace formula

$$A_C = \frac{1}{2} \sum_{i=1}^N (v_i^1 v_{i+1}^2 - v_{i+1}^1 v_i^2),$$

where $\vec{v}_{N+1} = \vec{v}_1$.

Proof.

An illustration supporting the proof is provided in 1, which is where the idea of the proof comes from. Without loss of generality, we may assume that all coordinates are positive. If this is not initially the case, the entire polygon can be translated into the positive quadrant without affecting its area.

For each $1 \leq i \leq N$ the edge $\vec{v}_i \vec{v}_{i+1}$ is associated with the area T_i of the trapeze that arises when connecting the line segment vertically with the x axis. The signed trapeze area of T_i can be computed with

$$T_i = \frac{1}{2}(v_i^2 + v_{i+1}^2)(v_i^1 - v_{i+1}^1).$$

Keep in mind that $\vec{x}_{N+1} = \vec{x}_1$.

The area T_i has a positive sign if $x_i \geq x_{i+1}$ (green arrow in Figure 1) and a negative

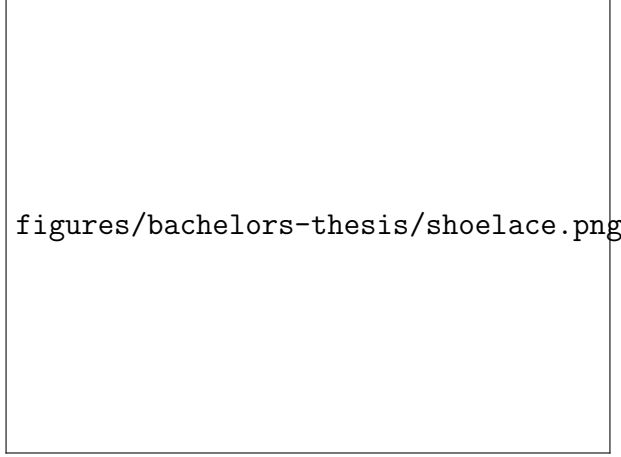


Figure 1: This figure shows a geometrical interpretation of the shoelace formula. In difference to the proposition, here the vertices are called P_i and not \vec{v}_i .
Source: [ShoelaceIllustration, 2022]

sign otherwise (red arrow). As depicted in the figure, the negatively signed areas precisely cancel the excess portions that would result from summing only the positively signed trapezoids. Thus the total polygon's area is equal to the sum of all trapezes

$$A_C = \sum_{i=1}^N T_i = \frac{1}{2} \sum_{i=1}^N (v_i^2 + v_{i+1}^2)(v_i^1 - v_{i+1}^1) = \frac{1}{2} \sum_{i=1}^N (v_i^1 v_{i+1}^2 - v_{i+1}^1 v_i^2).$$

□

With the Shoelace formula we are able to easily compute all cell areas at all times in the simulation. This enables us to implement the gradient flow over the area energy.

Definition 2.2. Area energy

The energy A_i , used to keep the cell i at a constant volume, reads

$$(1) \quad A_i(C_i) = \frac{1}{2} |A_i^d - A_{C_i}|^2,$$

where A_i^d is the desired cell area of cell i and A_{C_i} is the current cell area. If not stated otherwise, A_i^d is the initial area of the i th cell at the start of the simulation.

To maintain the cell area during the simulation, we evaluate the gradient flow of the area energy which indicates the direction of motion for each vertex for preserving the cell area.

Proposition 2.3. Area force

The gradient $\nabla_{\vec{v}_j^i} A_i(C_i)$ with respect to the j th vertex of cell i is given by

$$\nabla_{\vec{v}_j^i} A_i(C_i) = \frac{1}{2} (A_{C_i} - A_i^d) \begin{pmatrix} v_{j+1}^{i,2} - v_{j-1}^{i,2} \\ v_{j-1}^{i,1} - v_{j+1}^{i,1} \end{pmatrix},$$

where $\vec{v}_j^i = (v_j^{i,1}, v_j^{i,2})^T$.

Thus, the area force that gets applied on \vec{v}_j^i is given by

$$(2) \quad F_j^{(A_i)}(C_i) = -\nabla_{\vec{v}_j^i} A_i(C_i) = \frac{1}{2}(A_i^d - A_{C_i}) \begin{pmatrix} v_{j+1}^{i,2} - v_{j-1}^{i,2} \\ v_{j-1}^{i,1} - v_{j+1}^{i,1} \end{pmatrix}.$$

Proof.

For notational convenience, the subscript i is dropped, since the analysis focuses on a single cell. Choose $1 \leq j \leq N_V$. Let us first assume that $A^d \geq A_C$ to deal with the absolute value in the area energy. Then, we can compute

$$\begin{aligned} \nabla_{\vec{v}_j} A(C) &= \nabla_{\vec{v}_j} \frac{1}{2} |A^d - A_C|^2 \\ &= |A^d - A_C| \nabla_{\vec{v}_j} (A^d - A_C) \\ &= |A^d - A_C| \nabla_{\vec{v}_j} (-A_C) \\ &= |A^d - A_C| \nabla_{\vec{v}_j} \left(-\frac{1}{2} \sum_{k=1}^N (v_k^1 v_{k+1}^2 - v_{k+1}^1 v_k^2) \right) \\ &= -\frac{1}{2} |A^d - A_C| \begin{pmatrix} \partial_{v_j^1} (v_j^1 v_{j+1}^2 - v_j^1 v_{j-1}^2) \\ \partial_{v_j^2} (v_{j-1}^1 v_j^2 - v_{j+1}^1 v_j^2) \end{pmatrix} \\ &= -\frac{1}{2} |A^d - A_C| \begin{pmatrix} v_{j+1}^2 - v_{j-1}^2 \\ v_{j-1}^1 - v_{j+1}^1 \end{pmatrix} \end{aligned}$$

Remember that A^d is just an independent constant. In the other case, where $A^d < A_C$, there is just a change in the sign. Overall, we can write

$$\nabla_{\vec{v}_j} A(C) = -\frac{1}{2} (A^d - A_C) \begin{pmatrix} v_{j+1}^2 - v_{j-1}^2 \\ v_{j-1}^1 - v_{j+1}^1 \end{pmatrix}.$$

□

It is also valid to write $F_j^{(A_i)}(\vec{C})$ instead of $F_j^{(A_i)}(C_i)$, since C_i is included in \vec{C} . Figures 2 and 3 illustrate how the area force acts on a cell to either expand or contract it toward the desired target area.

2.2 Edge force

The next force we would like to model is the edge force. It acts on the cell's edges and aims to maintain their lengths. We define the edge $1 \leq j \leq N_V$ as

$$e_j = \overline{\vec{v}_j \vec{v}_{j+1}}$$

and we use the operator

$$E_C^j = \|\vec{v}_j - \vec{v}_{j+1}\|_2$$

figures/bachelors-thesis/forces/area1/area1.png

Figure 2: The figure displays the solution of Model Initially, the cell has an area of approximately 2.6. Arrows originating from each vertex represent the forces acting on the vertices at the corresponding time. The area force acts by pushing the vertices outward from the cell center, resulting in an increase in area. The computed areas at each time step are indicated below the respective diagrams. We can observe that the forces decrease as the actual cell area gets closer to its desired state. Once the target area of $A^d = 10.0$ is reached, the force vanishes and the system reaches a steady state.

figures/bachelors-thesis/forces/area2/area2.png

Figure 3: Similar to Figure 2, this image shows a cell that develops according to the area force. In contrast to the previous illustration, the initial area is now larger than the desired target area. As a result, the area force needs to reverse its direction to shrink the cell toward the target area $A^d = 10.0$. This outcome is consistently demonstrated across the four diagrams.

to compute the length of the edge.

The according energy for this edge is:

Definition 2.4. Edge energy

The energy $E_{i,j}$, used to keep the edge j of cell i at a constant length, reads

$$(3) \quad E_{i,j}(C_i) = \frac{1}{2} |E_{i,j}^d - E_{C_i}^j|^2,$$

where $E_{i,j}^d$ is the desired edge length of edge j in cell i and $E_{C_i}^j$ is the current edge length. If not stated otherwise, $E_{i,j}^d$ is the initial j th edge length of the i th cell at the start of the simulation.

Since each vertex v_j influences exactly the edge lengths of the edges e_j and e_{j-1} , we get the total edge force on v_j with:

Proposition 2.5. Edge force

The gradient $\nabla_{\vec{v}_j^i} E_j(C_i)$ with respect to the j th vertex of cell i is given by

$$\nabla_{\vec{v}_j^i} E_{i,j}(C_i) = \frac{E_{C_i}^j - E_{i,j}^d}{E_{C_i}^j} \begin{pmatrix} v_j^{i,1} - v_{j+1}^{i,1} \\ v_j^{i,2} - v_{j+1}^{i,2} \end{pmatrix},$$

where $\vec{v}_j^i = (v_j^{i,1}, v_j^{i,2})^T$.

The edge force acting on v_j^i in cell i is given by the formula

$$(4) \quad F_j^{(E_{i,j})}(C_i) = -\nabla_{\vec{v}_j^i} E_{i,j}(C_i) - \nabla_{\vec{v}_j^i} E_{i,j-1}(C_i)$$

$$(5) \quad = \frac{E_{i,j}^d - E_{C_i}^j}{E_{C_i}^j} \begin{pmatrix} v_j^{i,1} - v_{j+1}^{i,1} \\ v_j^{i,2} - v_{j+1}^{i,2} \end{pmatrix} + \frac{E_{i,j-1}^d - E_{C_i}^{j-1}}{E_{C_i}^{j-1}} \begin{pmatrix} v_{j-1}^{i,1} - v_j^{i,1} \\ v_{j-1}^{i,2} - v_j^{i,2} \end{pmatrix}$$

Proof.

We drop the i for the ease of notation. The computation is for the case $E_j^d \geq E_C^j$.

$$\begin{aligned} \nabla_{\vec{v}_j} E_j(C) &= \nabla_{\vec{v}_j} \left(\frac{1}{2} |E_j^d - E_C^j|^2 \right) \\ &= |E_j^d - E_C^j| \nabla_{\vec{v}_j} (E_j^d - E_C^j) \\ &= |E_j^d - E_C^j| (-\nabla_{\vec{v}_j} \|\vec{v}_j - \vec{v}_{j+1}\|_2) \\ &= |E_j^d - E_C^j| (-\nabla_{\vec{v}_j} [(v_j^1 - v_{j+1}^1)^2 + (v_j^2 - v_{j+1}^2)^2]^{\frac{1}{2}}) \\ &= |E_j^d - E_C^j| \left(-\frac{1}{2\|\vec{v}_j - \vec{v}_{j+1}\|_2} \nabla_{\vec{v}_j} [(v_j^1 - v_{j+1}^1)^2 + (v_j^2 - v_{j+1}^2)^2] \right) \\ &= |E_j^d - E_C^j| \left(-\frac{1}{2E_C^j} \begin{pmatrix} \partial_{v_j^1} (v_j^1 - v_{j+1}^1)^2 \\ \partial_{v_j^2} (v_j^2 - v_{j+1}^2)^2 \end{pmatrix} \right) \\ &= |E_j^d - E_C^j| \left(-\frac{1}{2E_C^j} \begin{pmatrix} 2(v_j^1 - v_{j+1}^1) \\ 2(v_j^2 - v_{j+1}^2) \end{pmatrix} \right) \\ &= -\frac{|E_j^d - E_C^j|}{E_C^j} \begin{pmatrix} v_j^1 - v_{j+1}^1 \\ v_j^2 - v_{j+1}^2 \end{pmatrix} \end{aligned}$$

figures/bachelors-thesis/forces/edge/edge1.png

Figure 4: The diagram illustrates the edge force acting on a DF cell. At time $t = 0$, the cell is shaped as a rectangle $[-3, 3] \times [-1, 1]$, giving horizontal edges a length of 6 and vertical edges a length of 2. The corresponding edge lengths at the different time steps are annotated below each diagram. The target configuration is the rectangle $[-1, 1] \times [-3, 3]$, implying that the horizontal edges need to contract while the vertical edges must stretch. This transformation is clearly observable in the progression of the diagrams.

To include the case $E_j^d < E_C^j$, where simply a sign change arises, we can drop the absolute value and write

$$\nabla_{\vec{v}_j} E_j(C) = \frac{E_C^j - E_j^d}{E_C^j} \begin{pmatrix} v_j^1 - v_{j+1}^1 \\ v_j^2 - v_{j+1}^2 \end{pmatrix}$$

to get the result.

□

An isolated application of the edge force can be seen in Figure 4.

2.3 Interior angle force

The combined application of the area and edge forces revealed instabilities in unfavorable configurations, where self-intersections of the cell edges occurred. Simulations without this energy sometimes can also result in constrictions at certain vertices, where the interior angle approaches 360. To address this issue, we introduce the interior angle energy.

The first challenge is to consistently determine the interior angle at a given vertex throughout the simulation. Although we could use \arccos to compute the angle, this method would suffer from poor stability as the angle approaches π or $-\pi$. A better alternative is to use the $\arctan2$ function, as it remains reliably stable for all angles.

Definition 2.6. $\arctan2$

The function

$$\arctan2 : \mathbb{R}^2 / \{0\} \rightarrow (-\pi, \pi]$$

is defined by:

$$\arctan2(x, y) = \begin{cases} \arctan(\frac{y}{x}) & x > 0 \\ \arctan(\frac{y}{x}) + \pi & x < 0, y > 0 \\ \arctan(\frac{y}{x}) - \pi & x < 0, y < 0 \\ \pi & x = 0, y > 0 \\ -\pi & x = 0, y < 0 \end{cases}.$$

The $\arctan2(y, x)$ function computes the angle of a vector $(x, y)^T$ with respect to the positive x axis.

With this, we can compute the angles

$$\begin{aligned} \theta_1 &= \arctan2(\vec{v}_{j-1} - \vec{v}_j), \\ \theta_2 &= \arctan2(\vec{v}_{j+1} - \vec{v}_j) \end{aligned}$$

between the positive x axis and the vector from \vec{v}_j to its neighboring vertices \vec{v}_{j-1} and \vec{v}_{j+1} . We get the wanted angle at \vec{v}_j by subtracting $\theta_2 - \theta_1$. To ensure that the angle lies within the interval $[0, 2\pi)$, we use the modulo operator $[\cdot]_{[0, 2\pi)}$, which repeatedly adds or subtracts 2π from the angle until it falls within the desired range. Thus, our interior angle operator is:

$$I_C^j = [\arctan2(\vec{v}_{j-1} - \vec{v}_j) - \arctan2(\vec{v}_{j+1} - \vec{v}_j)]_{[0, 2\pi)}.$$

With that, we can define our interior angle energy.

Definition 2.7. Interior angle energy

The energy associated with preserving the angle at vertex j of cell i is given by

$$I_{i,j}(C_i) = \frac{1}{2} |I_{i,j}^d - I_{C_i}^j|^2,$$

where $I_{i,j}^d$ is the desired interior angle at vertex j of cell i .

We continue by computing the resulting force. The function $\arctan2$ is partly defined and not truly differentiable. We still want to compute a gradient to use it for our interior angle force. Since $\arctan2(x, y) = \arctan(\frac{y}{x}) + \text{constant}$ almost everywhere, we just compute the gradient of $\arctan(\frac{y}{x})$ instead.

Another problem is the modulo operator $[\cdot]_{[0, 2\pi)}$, which is not differentiable at the interval limits. However, we just neglect the modulo operator as it does not affect the dynamics of the gradient.

Proposition 2.8. Interior angle force

The interior angle force that gets applied on vertex \vec{v}_j of cell i is given by

(6)

$$\begin{aligned}
F_j^{(I_{i,j})}(C_i) &= -\nabla_{\vec{v}_j}(I_{i,j-1}(C_i) + I_{i,j}(C_i) + I_{i,j+1}(C_i)) \\
&= (I_{C_i}^{j-1} - I_{i,j-1}^d) \left(-\frac{1}{\|\vec{v}_j - \vec{v}_{j-1}\|_2^2} \begin{pmatrix} v_j^2 - v_{j-1}^2 \\ v_{j-1}^1 - v_j^1 \end{pmatrix} \right) \\
&\quad + (I_{C_i}^j - I_{i,j}^d) \left(\frac{1}{\|\vec{v}_{j-1} - \vec{v}_j\|_2^2} \begin{pmatrix} v_{j-1}^2 - v_j^2 \\ v_j^1 - v_{j-1}^1 \end{pmatrix} - \frac{1}{\|\vec{v}_{j+1} - \vec{v}_j\|_2^2} \begin{pmatrix} v_{j+1}^2 - v_j^2 \\ v_j^1 - v_{j+1}^1 \end{pmatrix} \right) \\
&\quad + (I_{C_i}^{j+1} - I_{i,j+1}^d) \left(\frac{1}{\|\vec{v}_j - \vec{v}_{j+1}\|_2^2} \begin{pmatrix} v_j^2 - v_{j+1}^2 \\ v_{j+1}^1 - v_j^1 \end{pmatrix} \right)
\end{aligned}$$

Proof.

We are looking for

$$\nabla_{\vec{v}_j}(I_{i,j-1}(C_i) + I_{i,j}(C_i) + I_{i,j+1}(C_i))$$

as the vertex \vec{v}_j has an influence on the interior angles at the vertices \vec{v}_{j-1} , \vec{v}_j and \vec{v}_{j+1} .

Let us start with the computation of $\nabla_{\vec{v}_j} I_{i,j}(C_i)$. Similarly to the first forces, we get:

$$\begin{aligned}
\nabla_{\vec{v}_j} I_{i,j}(C_i) &= (I_{i,j}^d - I_{C_i}^j) \nabla_{\vec{v}_j} (-I_{C_i}^j) \\
&= (I_{i,j}^d - I_{C_i}^j) \nabla_{\vec{v}_j} [\arctan 2(\vec{v}_{j-1} - \vec{v}_j) - \arctan 2(\vec{v}_{j+1} - \vec{v}_j)]_{[0,2\pi)}.
\end{aligned}$$

At this point, the previously mentioned simplifications come into play and we use $\arctan(\frac{v_{j-1}^2 - v_j^2}{v_{j-1}^1 - v_j^1})$ instead of $\arctan 2(\vec{v}_{j-1} - \vec{v}_j)$ and neglect the modulo operator $[\cdot]_{[0,2\pi)}$.

In the next step, we need to compute the gradient

$$\nabla_{\vec{v}_j} \arctan\left(\frac{v_{j-1}^2 - v_j^2}{v_{j-1}^1 - v_j^1}\right).$$

Therefore, we define helper functions

$$f(x, y) = \arctan\left(\frac{y}{x}\right)$$

and

$$g(\vec{v}_{j-1}, \vec{v}_j) = \begin{pmatrix} v_{j-1}^1 - v_j^1 \\ v_{j-1}^2 - v_j^2 \end{pmatrix}.$$

With these helper functions, we can write

$$\arctan\left(\frac{v_{j-1}^2 - v_j^2}{v_{j-1}^1 - v_j^1}\right) = (f \circ g)(\vec{v}_{j-1}, \vec{v}_j)$$

and use the two dimensional chain rule to stepwise compute the searched gradient.

$$\begin{aligned}
\frac{\partial f(x, y)}{\partial x} &= \frac{1}{1 + \frac{y^2}{x}} \left(-\frac{y}{x^2} \right) = -\frac{y}{x^2 + y^2}, \\
\frac{\partial f(x, y)}{\partial y} &= \frac{1}{1 + \frac{y^2}{x}} \frac{1}{x} = \frac{x}{x^2 + y^2}, \\
\nabla_{v_j^1} g(\vec{v}_{j-1}, \vec{v}_j) &= (-1, 0)^T, \\
\nabla_{v_j^2} g(\vec{v}_{j-1}, \vec{v}_j) &= (0, -1)^T.
\end{aligned}$$

With that, we can compute:

$$\begin{aligned}
\frac{\partial(f \circ g(\vec{v}_{j-1}, \vec{v}_j))}{\partial v_j^1} &= (\nabla f \circ g(\vec{v}_{j-1}, \vec{v}_j)) \cdot \nabla_{v_j^1} g(\vec{v}_{j-1}, \vec{v}_j) \\
&= \begin{pmatrix} -\frac{v_{j-1}^2 - v_j^2}{(v_{j-1}^1 - v_j^1)^2 + (v_{j-1}^2 - v_j^2)^2} \\ \frac{v_{j-1}^1 - v_j^1}{(v_{j-1}^1 - v_j^1)^2 + (v_{j-1}^2 - v_j^2)^2} \end{pmatrix} \cdot \begin{pmatrix} -1 \\ 0 \end{pmatrix} \\
&= \frac{v_{j-1}^2 - v_j^2}{(v_{j-1}^1 - v_j^1)^2 + (v_{j-1}^2 - v_j^2)^2} \\
&= \frac{v_{j-1}^2 - v_j^2}{\|\vec{v}_{j-1} - \vec{v}_j\|_2^2}
\end{aligned}$$

And similarly:

$$\begin{aligned}
\frac{\partial(f \circ g(\vec{v}_{j-1}, \vec{v}_j))}{\partial v_j^2} &= (\nabla f \circ g(\vec{v}_{j-1}, \vec{v}_j)) \cdot \nabla_{v_j^2} g(\vec{v}_{j-1}, \vec{v}_j) \\
&= \begin{pmatrix} -\frac{v_{j-1}^2 - v_j^2}{(v_{j-1}^1 - v_j^1)^2 + (v_{j-1}^2 - v_j^2)^2} \\ \frac{v_{j-1}^1 - v_j^1}{(v_{j-1}^1 - v_j^1)^2 + (v_{j-1}^2 - v_j^2)^2} \end{pmatrix} \cdot \begin{pmatrix} 0 \\ -1 \end{pmatrix} \\
&= -\frac{v_{j-1}^1 - v_j^1}{(v_{j-1}^1 - v_j^1)^2 + (v_{j-1}^2 - v_j^2)^2} \\
&= \frac{v_j^1 - v_{j-1}^1}{\|\vec{v}_{j-1} - \vec{v}_j\|_2^2}
\end{aligned}$$

Overall, we get

$$\nabla_{\vec{v}_j} \arctan\left(\frac{v_{j-1}^2 - v_j^2}{v_{j-1}^1 - v_j^1}\right) = \frac{1}{\|\vec{v}_{j-1} - \vec{v}_j\|_2^2} \begin{pmatrix} v_{j-1}^2 - v_j^2 \\ v_j^1 - v_{j-1}^1 \end{pmatrix}.$$

figures/bachelors-thesis/forces/angle/angle1.png

Figure 5: The figure illustrates the action of the interior angle force on the vertices of a DF cell. The initial state, shown in the first plot, must be mirrored horizontally to achieve the desired state depicted in the final plot. This reshaping shows on the one hand that the dynamic is capable of decreasing interior angles from 270° to 90° and on the other hand it can also increase interior angles from 90° to 270° . Below each chart, we can see the current interior angles of the two vertices that have the y value zero.

Thus, we can come back to:

$$\begin{aligned}\nabla_{\vec{v}_j} I_{i,j}(C_i) &= (I_{i,j}^d - I_{C_i}^j) \nabla_{\vec{v}_j} \left(\arctan\left(\frac{v_{j-1}^2 - v_j^2}{v_{j-1}^1 - v_j^1}\right) - \arctan\left(\frac{v_{j+1}^2 - v_j^2}{v_{j+1}^1 - v_j^1}\right) \right) \\ &= (I_{i,j}^d - I_{C_i}^j) \left(\frac{1}{\|\vec{v}_{j-1} - \vec{v}_j\|_2^2} \begin{pmatrix} v_{j-1}^2 - v_j^2 \\ v_{j-1}^1 - v_j^1 \end{pmatrix} - \frac{1}{\|\vec{v}_{j+1} - \vec{v}_j\|_2^2} \begin{pmatrix} v_{j+1}^2 - v_j^2 \\ v_{j+1}^1 - v_j^1 \end{pmatrix} \right)\end{aligned}$$

For the neighboring vertices, we get

$$\begin{aligned}\nabla_{\vec{v}_j} I_{i,j-1}(C_i) &= (I_{i,j-1}^d - I_{C_i}^{j-1}) \nabla_{\vec{v}_j} \left(\arctan\left(\frac{v_{j-2}^2 - v_{j-1}^2}{v_{j-2}^1 - v_{j-1}^1}\right) - \arctan\left(\frac{v_j^2 - v_{j-1}^2}{v_j^1 - v_{j-1}^1}\right) \right) \\ &= (I_{i,j-1}^d - I_{C_i}^{j-1}) \left(0 - \frac{1}{\|\vec{v}_j - \vec{v}_{j-1}\|_2^2} \begin{pmatrix} v_j^2 - v_{j-1}^2 \\ v_j^1 - v_{j-1}^1 \end{pmatrix} \right)\end{aligned}$$

and

$$\begin{aligned}\nabla_{\vec{v}_j} I_{i,j+1}(C_i) &= (I_{i,j+1}^d - I_{C_i}^{j+1}) \nabla_{\vec{v}_j} \left(\arctan\left(\frac{v_j^2 - v_{j+1}^2}{v_j^1 - v_{j+1}^1}\right) - \arctan\left(\frac{v_{j+2}^2 - v_{j+1}^2}{v_{j+2}^1 - v_{j+1}^1}\right) \right) \\ &= (I_{i,j+1}^d - I_{C_i}^{j+1}) \left(\frac{1}{\|\vec{v}_j - \vec{v}_{j+1}\|_2^2} \begin{pmatrix} v_j^2 - v_{j+1}^2 \\ v_j^1 - v_{j+1}^1 \end{pmatrix} - 0 \right).\end{aligned}$$

The sum of these three gradients is equal to the force stated in the proposition. \square

Figure 5 illustrates the isolated effect of the interior angle force.

2.4 Overlap force

Unlike the previous energies, which act independently on each cell, the overlap force is the first to account for interactions between multiple cells, thereby introducing

cell-to-cell interaction into the simulation.

The challenging aspect of computing the overlap force lies in detecting overlaps within the cell system. An overlap is treated as a DF cell in its own right, composed of the vertices from each of the two overlapping cells that lie inside the other, along with the two intersection points where the cell boundaries intersect.

Once all overlaps have been identified, we apply a dynamic similar to that of the area force—but with a desired area of zero. This generates a force that acts to eliminate the overlap by reducing its area to zero. The resulting force is then applied to the vertices of the original cells that define the overlapping region.

The first step in detecting overlaps is identifying the intersection points between cell boundaries. Intersections can be identified by representing the cell edges as line segments and computing the intersection points between segments belonging to different cells.

Having found all intersections, we can apply the following algorithm, that can be used to compute all overlaps between two cells.

Algorithm 2.9. *Computation of a discrete overlap*

INPUT:

- *Discrete cells C and ζ*
- *List I of unused intersections of C and ζ*

```

function CONSTRUCTOVERLAP( $C, \zeta, I$ )
   $usedIntersections = List\{Intersection\}(I[1])$ 
   $newOverlap = List\{Vertices\}(I[1])$ 
   $currentIntersection = I[1]$ 
  for  $counter = 1 : length(I)$  do
    if  $counter$  is even then
       $newPath, newIntersection = findPath(currentIntersection, C, I)$ 
    else
       $newPath, newIntersection = findPath(currentIntersection, \zeta, I)$ 
    end if
     $append!(newOverlap, newPath)$ 
    if  $newIntersection == I[1]$  then
      return  $newOverlap, usedIntersections$ 
    else
       $append!(newOverlap, newIntersection)$ 
       $append!(usedIntersections, newIntersection)$ 
       $currentIntersection = newIntersection$ 
    end if
  end for
end function

```

OUTPUT:

- *A single intersection ‘newOverlap’ which occurs between C and ζ and which uses vertices from C and ζ as well as only intersections from I*
- *A list ‘usedIntersections’ of all intersection that are used in ‘newOverlap’*

The algorithm begins by selecting the first intersection point $I[1]$ from the list I as the initial vertex of the overlap cell ‘newOverlap’. This point is also added to the list ‘usedIntersections’.

Next, the function ‘getOverlap’ calls another function, ‘findPath’, which determines the path along the discrete cell ζ from the current intersection point to the next intersection in I encountered while traversing the edges of ζ . This next intersection is also returned by the function. The identified path is a list of vertices in ζ that lie strictly between the two intersections. It may be empty if the next intersection occurs on the same edge as the current one. Both the path and the newly found intersection are appended to ‘newOverlap’, and the intersection is also added to the list usedIntersections.

Since each intersection implies changing the cell from which the overlapping cell uses the edges, ‘findPath’ is now applied to the other cell. Again, it will deliver the next intersection as well as a list of the in between laying vertices. The vertex list always gets appended to ‘newOverlap’.

If the newly found intersection is equal to the initial intersection $I[1]$, then the construction of the discrete overlap cell ‘newOverlap’ is complete. At this point, both ‘newOverlap’ and ‘usedIntersections’ can be returned by the function ‘constructOverlap’.

Otherwise, the newly found intersection is appended to both ‘newOverlap’ and ‘usedIntersections’, and the process continues by calling ‘findPath’ on the other discrete cell. This step is repeated until the starting intersection is reached, completing the overlap cell construction.

Once an overlap between C and ζ has been successfully extracted, all intersections used in its construction can be removed from the list I , since each intersection point belongs to exactly one overlap. As long as I is not empty, the function ‘constructOverlap’ can be called again with the updated list to extract the next overlap. When I is empty, we can be certain that all intersections between C and ζ have been processed, and thus all overlaps between the two cells have been identified.

Each time ‘findPath’ is called, it is not immediately clear in which direction the function should traverse the vertices of the given cell. However, the correct direction can be determined using the following approach.

Starting from the current intersection passed into the function, move a small distance in one direction along the edge of the given cell where the intersection is located. Next, check whether this new point lies within the boundaries of the other cell as well. If the point is found in both cells, the chosen direction is correct. If not, then the opposite direction must be used.

A simple method to determine whether a point lies inside a polygon is to draw a ray from the point to the outside of the polygon. The number of intersections between the ray and the polygon’s edges determines the point’s position. If the number of intersections is odd, the point is inside the polygon. If it is even, the point is outside the polygon.

After introducing the method for detecting overlaps, we can now define the overlap force, which acts on the cell vertices involved in an overlap. This force is first

computed based on the geometry of the overlap and then distributed to the corresponding vertices of the original cells.

Definition 2.10. Overlap energy

Let C_i and C_k be two cells from the system \vec{C} and $\Omega_{i,k}$ be the set of all overlaps that appear between C_i and C_k , like explained above. Then, the overlap energy of C_i is given by the formula

$$(7) \quad O_i(\vec{C}) = \sum_{k=1, k \neq i}^{N_C} \left(\sum_{D_l \in \Omega_{i,k}} \frac{1}{2} |A_{D_l}|^2 \right),$$

where A_{D_l} is the area of the overlap D_l .

To maintain the cell area during the simulation, we evaluate the gradient flow of the area energy which indicates the direction of motion for each vertex for preserving the cell area.

Proposition 2.11. Overlap force

The overlap force that acts on the vertex \vec{v}_j of cell i is given by

$$(8) \quad F_j^{O_i}(\vec{C}) = \sum_{k=1, k \neq i}^{N_C} \left(\sum_{D_l \in \Omega_{i,k}} \frac{1}{2} A_{D_l} \begin{pmatrix} d_{j+1}^{D_l,2} - d_{j-1}^{D_l,2} \\ d_{j-1}^{D_l,1} - d_{j+1}^{D_l,1} \end{pmatrix} \right),$$

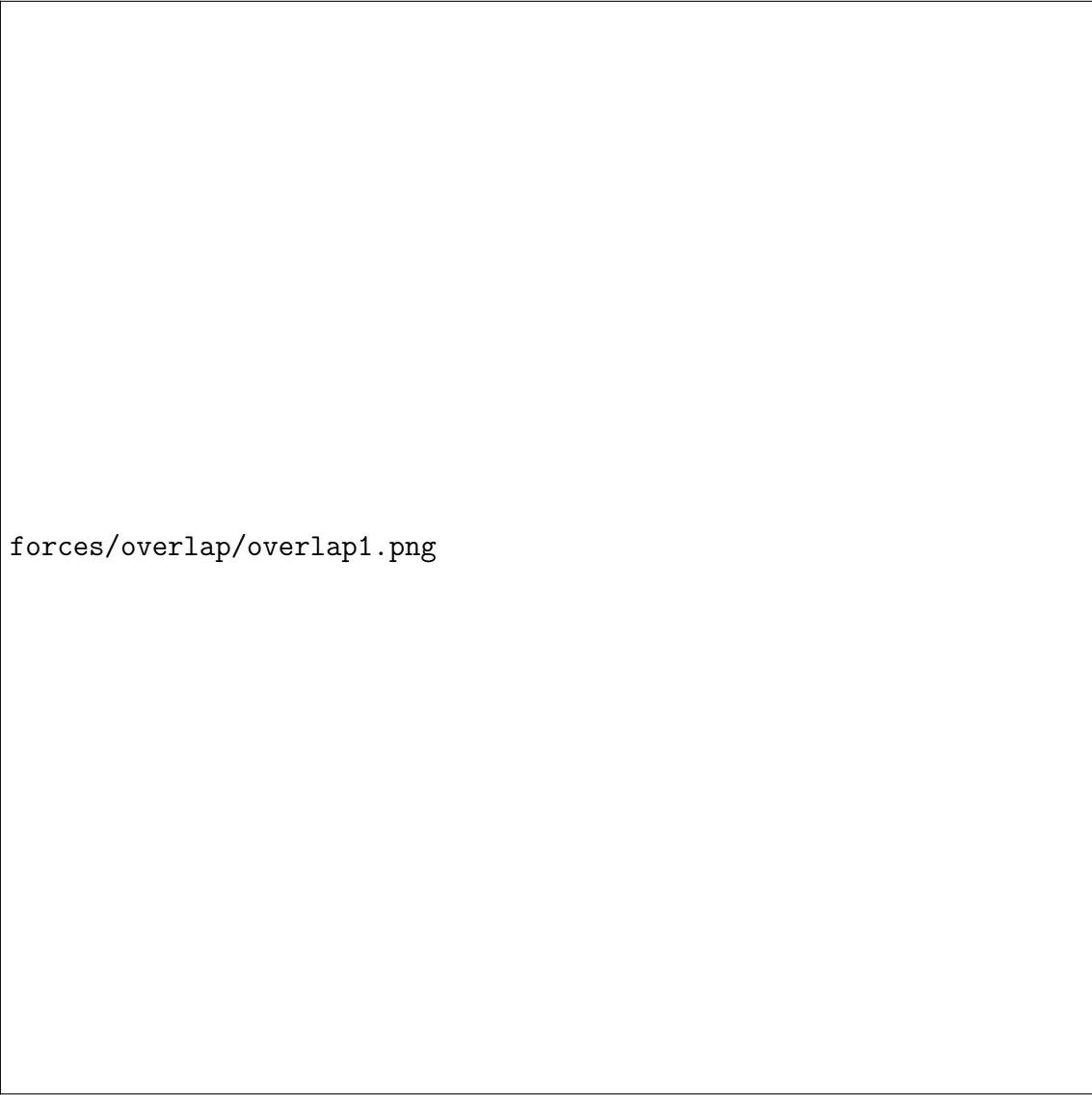
where $\Omega_{i,k}$ is the set of all overlaps that arise between the cells i and k , $\vec{d}_{j-1}^{D_l} = (d_{j-1}^{D_l,1}, d_{j-1}^{D_l,2})^T$ and $\vec{d}_{j+1}^{D_l} = (d_{j+1}^{D_l,1}, d_{j+1}^{D_l,2})^T$ are the neighboring vertices of \vec{v}_j in the overlap D_l and A_{D_l} is the area of the overlap D_l .

Proof.

The formula arises from the sums from the overlap energy and the gradient from the area force in Proposition 2.3, where the desired area is set to zero.

Figure 6 illustrates the interaction between two overlapping cells, highlighting the effect of the overlap force on their vertices.

2.5 A simulation run



forces/overlap/overlap1.png

Figure 6: This figure demonstrates how the overlap force acts on two overlapping DF cells. The blue arrows indicate the forces acting on the blue cell, while the red arrows represent those acting on the red cell. The current overlap areas at each time step are displayed below the corresponding diagrams. On each consecutive diagram, we can see that the overlap gets reduced, until the area of the overlap is zero.

3 Sanity check

Having introduced our cell dynamics, we now want to take a look at the simulation results. Therefore, we aim to compare our simulation results to results from an established cell model from [Bruna and Chapman, 2012]. In [Bruna and Chapman, 2012] the diffusion dynamics of first a point particle model and second a hard sphere model is studied. Thereby, the two density distributions:

- the joint probability density function $P(\vec{X}, t)$ of the system of all cell centres \vec{X} at time t ,
- the marginal distribution function of the first particle $p(\vec{x}_1, t)$

play an important roll.

The joint probability density function $P(\vec{X}, t)$ is a function describing the positions of all particles in the system, while the marginal distribution function $p(\vec{x}_1, t)$ is a function describing only the position of the first particle.

It is sufficient to consider only the marginal distribution function of first particle, because all particle act similarly.

Gaining $p(\vec{x}_1, t)$ from $P(\vec{X}, t)$ is a big reduction of complexity, since we reduce from a high-dimensional PDE for P to a low-dimensional PDE for p .

The most simple model that gets considered for the diffusion dynamics of cell systems is the point particle model. Here the cells get modeled with sizeless points that perform a Brownian motion on the domain.

Since the cells do not have a real size, no interaction between the cells can occur, since they will never hit upon each other.

The paper [Bruna and Chapman, 2012] analyses these dynamics on the domain

$$\Omega_{BC} = [-0.5, 0.5]^2,$$

on which $N_{BC} = 400$ particles are located.

The movement of each point particle \vec{x}_i in the simulation is given by the SDE

$$d\vec{x}_i(t) = \sqrt{2}dB_t^{(i)}, \quad 1 \leq i \leq N_{BC},$$

which describes a Brownian motion in Ω_{BC} . The reflective boundary condition on $\partial\Omega_{BC}$ is imposed. It is known, that the joint probability density of the particle system in this setup evolves according to the diffusion equation, i.e.

$$(9) \quad \frac{\partial P}{\partial t}(\vec{X}, t) = \Delta_{\vec{X}} P = \nabla_{\vec{X}} \cdot [\nabla_{\vec{X}} P]$$

inside of the domain.

Since all particles are uncorrelated, we can compute

$$(10) \quad P(\vec{X}) = \prod_{i=1}^{N_{BC}} p(\vec{x}_i, t).$$

The marginal distribution function the of first particle can then be determined via

$$p(\vec{x}_1, t) = \int P(\vec{X}, t) d\vec{x}_2 \dots d\vec{x}_{N_{BC}}.$$

A next step that results in the hard sphere cell model (HSCM) is to give the cell particles a real size.

Let $0 < \epsilon \ll 1$ be the diameter of all cells that are now two dimensional discs with the same size. This changes the dynamics of the cells immense, since they now have chance to collide into each other which is a form of interaction.

The authors of [Bruna and Chapman, 2012] also did a simulation with the HSCM. The setting is as similar as possible to the point particle model, because a main goal of the paper was to compare the diffusion characteristics of both models. There are still $N_{BC} = 400$ cells located on the domain.

The initial condition of both models follows a two dimensional normal distribution with the addition that the distance of each cell centre to all others is at least ϵ . The used distribution $\mathcal{N}_2\left(\begin{pmatrix} 0 \\ 0 \end{pmatrix}, \begin{pmatrix} 0.09^2 & 0 \\ 0 & 0.09^2 \end{pmatrix}\right)$ has an integral of one over Ω_{BC} .

We can compute this initial condition with Algorithm 3.1.

Algorithm 3.1. *Computation of the initial cell system*

1. Generate a point $\vec{x} \sim \mathcal{N}_2\left(\begin{pmatrix} 0 \\ 0 \end{pmatrix}, \begin{pmatrix} 0.09^2 & 0 \\ 0 & 0.09^2 \end{pmatrix}\right)$.
2. If for all already generated centres $\vec{x}_j : \|\vec{x} - \vec{x}_j\|_2 > \epsilon$ is true, use \vec{x} as the next cell centre, otherwise discard the point and restart with step 1 until N_{BC} cell centres are found.

Since we do not want any overlap to occur during the whole simulation with the HSCM, the feasible domain for the whole cell system is not directly $\Omega_{BC}^{N_{BC}}$, but instead

$$\Omega_{BC}^\epsilon = \Omega_1^\epsilon \times \dots \times \Omega_{N_{BC}}^\epsilon, \\ \Omega_i^\epsilon = \Omega_{BC} \setminus (\cup_{j \neq i} B_\epsilon(\vec{x}_j)), \quad 1 \leq i \leq N_{BC},$$

where $B_\epsilon(\vec{x}_j)$ denotes the ball around \vec{x}_j with radius ϵ .

This domain prevents overlaps between the cells by not allowing each cell to drift closer than ϵ to any other cell.

HSCM cells perform the same Brownian motion as the point particles.

The next question is, how cell collisions are modelled. Unlike in our DCF model where cell interactions are modelled as forces acting inside of the domain, the cell collisions from the HSCM arise from the reflective boundary condition.

Let us assume that two cells i and j are given such that $\|\vec{x}_i - \vec{x}_j\|_2 = \epsilon$ is true. Then, both cell centres are located at the boundary $\partial\Omega_{BC}^\epsilon$. Here, the reflective boundary condition is still imposed and it causes both cells to bounce off from each other in the direction of the outward normal vector from the excluded area of the respectively other cell.

In [Bruna and Chapman, 2012] the authors managed to compute the marginal distribution function of the first particle of the HSCM. In two dimensions it is given by:

$$(11) \quad \frac{\partial p}{\partial t}(\vec{x}_1, t) = \nabla_{\vec{x}_1} \cdot \left\{ \nabla_{\vec{x}_1} \left[p + \frac{\pi}{2} (N_{BC} - 1) \epsilon^2 p^2 \right] \right\}.$$

We can see a connection to Equation 9. Let us look at the differential equation

$$\frac{\partial P}{\partial t}(\vec{X}, t) = \nabla_{\vec{X}} \cdot [D_{\epsilon}(p) \nabla_{\vec{X}} P], \quad D_{\epsilon}(p) = 1 + \frac{\pi}{2}(N_{BC} - 1)\epsilon^2 p \text{ ???}.$$

For $\epsilon = 0$ we can then see that $D_{\epsilon}(p) = 1$ and Equation 9 is given. If $\epsilon > 0$ on the other hand, we have that $D_{\epsilon}(p) \geq 1$ and we get Equation 11.

Thus, we have a higher diffusion rate for $\epsilon > 0$. In that case, we can see that the diffusivity increases with either:

- (a) a larger N_{BC} which would mean more interacting cells,
- (b) a larger ϵ that leads to a higher interaction radius per cell,
- (c) a locally higher cell concentration p .

Overall, we conclude that the bounce effect of the HSCM enhances the diffusion rate of the system's density.

Another evidence of this behavior is shown in Figure 2 in [Bruna and Chapman, 2012]. This figure contains the following four plots:

- (a) shows the solution of the linear diffusion equation 9 for point particles.
- (b) shows the histogram of a Monte Carlo simulation of the point particle model.
- (c) shows the solution of the nonlinear diffusion equation 11 for finite-sized particles.
- (d) shows the histogram of a Monte Carlo simulation of the HSCM.

In a Monte Carlo simulation, a stochastic process is simulated many times in order to analyse whether the results follow a specific stochastic distribution. In our case that specific stochastic distribution is the density

* 400 particles/cells * initial distribution $N(0, 0.09)$ + no overlaps for hard discs
The domain of the system is

a square with side length 1 around the origin and the time step size is 10^{-5} .

Figure 2 in [Bruna and Chapman, 2012] shows the marginal distribution function $p(x_1, t)$ at time $t = 0.05$. The figure compares the solution of the nonlinear diffusion equation (11) for finite-sized particles with the solution of the linear diffusion equation (4) for point particles.

The figure consists of four plots:

The figure is a useful tool for understanding the behavior of the system and the effects of excluded-volume interactions on the collective diffusion rate. The the heat equation and Equation (4) and in Figure 2a and 2c show similar characteristics as the stochastic simulations in 2b and 2d. We can observe that the excluded-volume effects enhance the overall collective diffusion rate.

Statement of authorship

I hereby declare that I have written this thesis (*Diffusitivity of deformable cells*) under the supervision of Jun.-Prof. Dr. Markus Schmidtchen independently and have listed all used sources and aids. I am submitting this thesis for the first time as part of an examination. I understand that attempted deceit will result in the failing grade „not sufficient“ (5.0).

Tim Vogel
Dresden, May 2, 2025
Technische Universität Dresden
Matriculation Number: 4930487

References

- [Bruna and Chapman, 2012] Bruna, M. and Chapman, S. J. (2012). Excluded-volume effects in the diffusion of hard spheres. *Phys. Rev. E*, 85:011103.
- [ShoelaceIllustration, 2022] ShoelaceIllustration (2022). Deriving the trapezoid formula. URL: <https://commons.wikimedia.org/wiki/File:Trapez-formel-prinz.svg>. Published by user 'Ag2gaeh'. Last accessed on 23.11.2023.
- [Vogel, 2023] Vogel, T. (2023). Modelling of cells and their dynamics.